

磁場と光子場の中で発達する 電磁力スケード

岡山商科大

中塚隆郎

共同研究

岡山理科大学、川崎医科大学、JAXA

Contents

- 宇宙カスケードの特色
- 詳しい断面積と宇宙カスケードの数値積分解
- 簡略化断面積と光子ガス中のカスケードの解析解
- 簡略化断面積と磁場中のカスケードの解析解
- 磁場中のカスケードが見えるか？
- シャワーの解析解による開発プログラムの点検
- 結論と議論

Comparison of the cross-sections

	radiation $\Phi(E, v)dv$	pair $\Psi(W, u)du$
in matter	$\frac{1}{X_0} \phi(E, v)dv$	$\frac{1}{X_0} \psi(W, u)du$
in photon gas	$\frac{1}{X_P} \frac{\phi(\kappa, v)}{E/W_0} dv$	$\frac{1}{X_P} \frac{\psi(\lambda, u)}{W/W_0} du$
in magnetic field	$\frac{1}{X_M} \frac{\phi(E, v)}{(E/W_0)^{1/3}} dv$	$\frac{1}{X_M} \frac{\psi(W, u)}{(W/W_0)^{1/3}} du$

where

$$u \equiv W/E \quad \text{and} \quad v \equiv E/W$$

and

$$X_0^{-1} = 4\alpha(N/A)Z^2 r_0^2 \ln(183Z^{-1/3})$$

$$X_P^{-1} = (3\sigma_T/4)n_0/\kappa_0$$

$$X_M^{-1} = \left\{ 3.9 \times 10^6 (H/H_c)^{2/3} \text{GeV}^{1/3}/cm \right\} / W_0^{1/3}, \quad \text{with } H_c = 4.41 \times 10^{13} G$$

光子ガスでの断面積の中の同次関数

Homogenous functions, $\phi(\kappa, v)$ and $\psi(\lambda, u)$, of the cross-section for Inverse Compton (left) and photon-photon pair production (right) are indicated below:

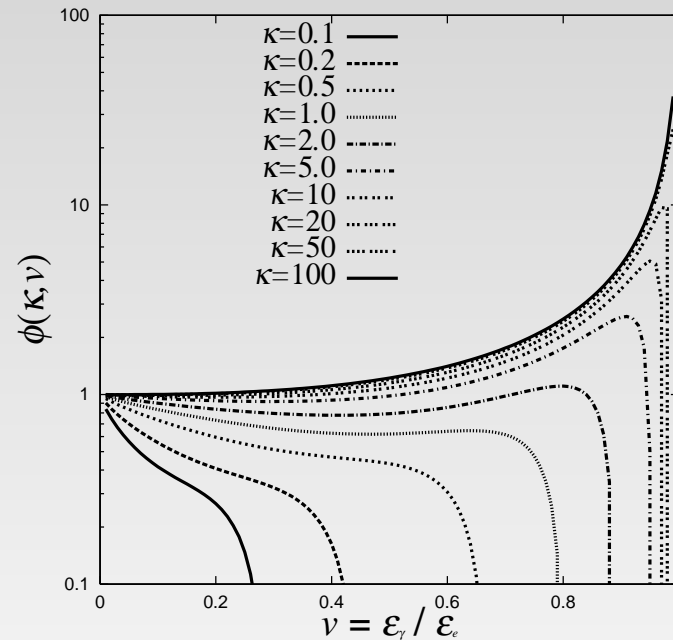


Figure 1: $\kappa \equiv \omega_0 \varepsilon_e = .1, .2, .5, \dots, 100$, from left to right.

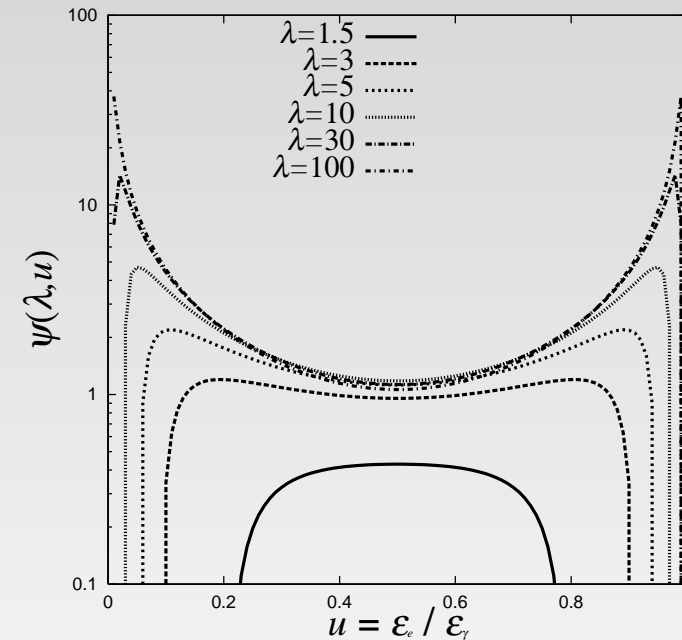
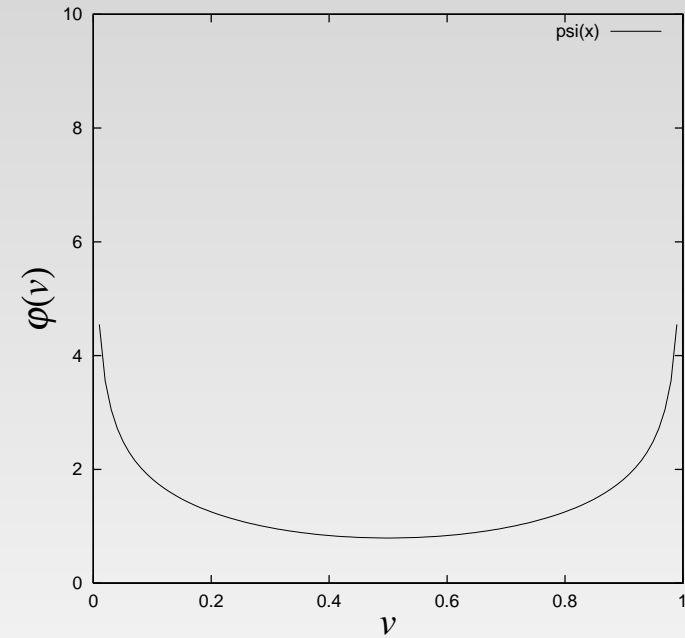
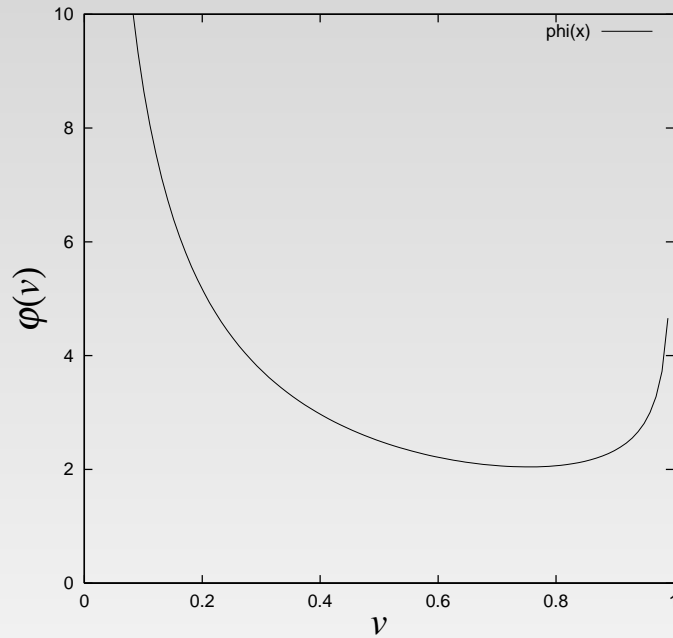


Figure 2: $\lambda \equiv \omega_0 \varepsilon_\gamma = .1, .2, .5, \dots, 100$, from bottom to top.

磁場での断面積の中の同次関数

Homogenous functions, $\phi(E, v)$ and $\psi(W, u)$, of the cross-section for photon radiation (left) and pair production (right) under the magnetic fields are indicated below:



Figure

$$\phi(v) = \frac{1 + (1 - v)^2}{v^{2/3}(1 - v)^{1/3}}.$$

3:

Figure

$$\psi(u) = \frac{u^2 + (1 - u)^2}{u^{1/3}(1 - u)^{1/3}}.$$

4:

数値積分法で得たカスケードの遷移曲線

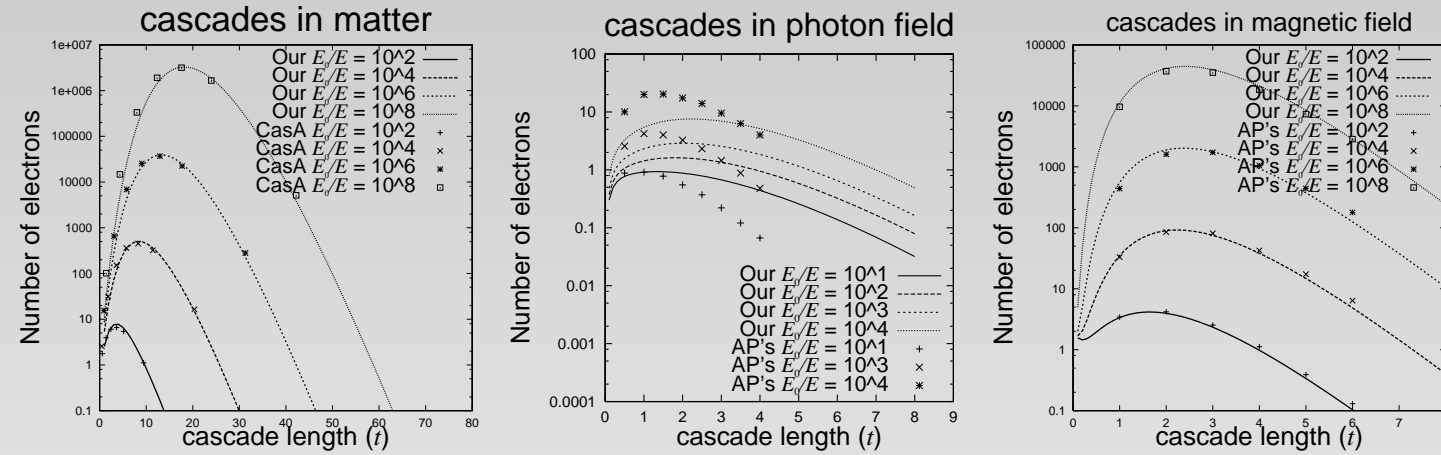


Figure 5: Transition curves of shower electron developing in matter (left), photon fields (middle), and magnetic fields (right). Our results in matter (lines) are compared with the analytical results in Nishimura, and our results in photon fields with $\kappa_0 = 10^3$ and in magnetic fields with cascade length defined by $3.9 \times 10^6 (\frac{H}{H_c})^{\frac{2}{3}} \frac{x}{cm} / (\frac{W_0}{GeV})^{\frac{1}{3}}$ (lines) are compared with those indicated in Aharonian and Plyasheshnikov (dots).

Cascades in photon gas

Diffusion equation

$$\begin{aligned}\frac{d}{\kappa_0 dt} \pi(\kappa, t) &= -\frac{\pi(\kappa)}{\kappa} \int_0^1 \phi(\kappa, v) dv + \int_{\kappa}^1 \phi(\kappa', 1 - \frac{\kappa}{\kappa'}) \frac{\pi(\kappa')}{\kappa'} \frac{d\kappa'}{\kappa'} \\ &\quad + 2 \int_{\kappa}^1 \psi(\lambda', \frac{\kappa}{\lambda'}) \frac{\gamma(\lambda')}{\lambda'} \frac{d\lambda'}{\lambda'}, \\ \frac{d}{\kappa_0 dt} \gamma(\lambda, t) &= \int_{\lambda}^1 \phi(\kappa', \frac{\lambda}{\kappa'}) \frac{\pi(\kappa')}{\kappa'} \frac{d\kappa'}{\kappa'} - \frac{\gamma(\lambda)}{\lambda} \int_0^1 \psi(\lambda, u) du,\end{aligned}$$

for the differential energy spectra, $\pi(\kappa, t)$ and $\gamma(\lambda, t)$, with

$$\kappa \equiv \omega_0 \varepsilon_e \quad \text{and} \quad \lambda \equiv \omega_0 \varepsilon_{\gamma},$$

where ε_e , ε_{γ} , and ω_0 denote the energies of the shower electron, shower photon, and background photon in units of mc^2 , and κ_0 denotes κ or λ of the incident particle.

Approximating the homogenous functions

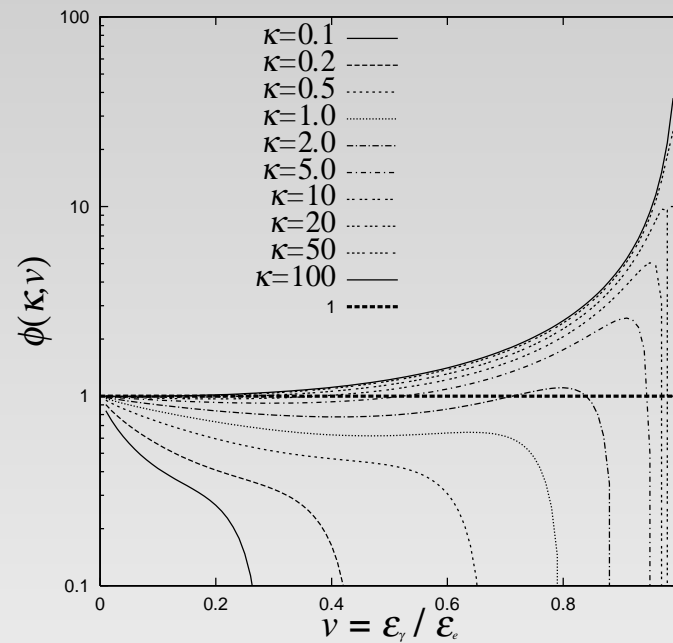


Figure 6: $\phi(\kappa, v) \simeq 1$.

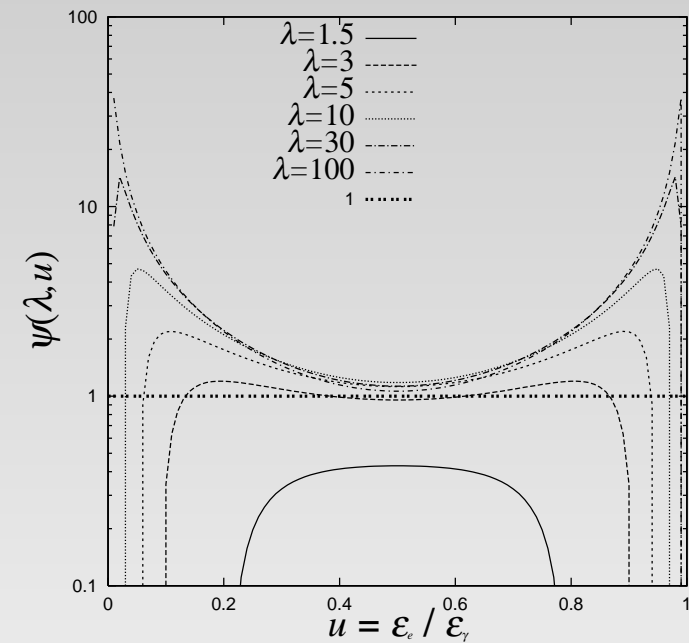


Figure 7: $\psi(\lambda, u) \simeq 1$.

Applying Mellin transforms

$$\begin{pmatrix} \mathcal{M}(s, t) \\ \mathcal{N}(s, t) \end{pmatrix} \equiv \int_0^\infty d\kappa \left(\frac{\kappa}{\kappa_0} \right)^s \begin{pmatrix} \pi(\kappa, t) \\ \gamma(\kappa, t) \end{pmatrix},$$

we have the differential-difference equations,

$$\frac{\partial}{\partial t} \begin{pmatrix} \mathcal{M}(s, t) \\ \mathcal{N}(s, t) \end{pmatrix} = R(s) \begin{pmatrix} \mathcal{M}(s - 1, t) \\ \mathcal{N}(s - 1, t) \end{pmatrix}$$

with

$$R(s) \equiv \begin{pmatrix} -s/(s + 1) & 2/(s + 1) \\ 1/(s + 1) & -1 \end{pmatrix},$$

and the differential spectra of shower particles become

$$\begin{pmatrix} \pi(\kappa, t) \\ \gamma(\kappa, t) \end{pmatrix} \equiv \frac{1}{2\pi i} \int_{\sigma-i\infty}^{\sigma+i\infty} ds \frac{\kappa_0^s}{\kappa^{s+1}} \begin{pmatrix} \mathcal{M}(s, t) \\ \mathcal{N}(s, t) \end{pmatrix}.$$

We derive the approximated solution by dividing t with n equal stepsizes,
 $\Delta t \equiv t/n$,

$$\begin{pmatrix} \mathcal{M}_k(s) \\ \mathcal{N}_k(s) \end{pmatrix} = \begin{pmatrix} \mathcal{M}_{k-1}(s) \\ \mathcal{N}_{k-1}(s) \end{pmatrix} + R(s) \begin{pmatrix} \mathcal{M}_{k-1}(s-1) \\ \mathcal{N}_{k-1}(s-1) \end{pmatrix} \Delta t, \\ k = 1, 2, \dots, n,$$

with $\mathcal{M}_0(s) = 0$ and $\mathcal{N}_0(s) = 1$. Then we have

$$\begin{pmatrix} \mathcal{M}_n(s) \\ \mathcal{N}_n(s) \end{pmatrix} = \sum_{k=0}^n {}_n C_k \left(\frac{t}{n} \right)^k R^{[k]}(s) \begin{pmatrix} \mathcal{M}_0(s-k) \\ \mathcal{N}_0(s-k) \end{pmatrix},$$

where

$$R^{[0]}(s) \equiv 1 \quad \text{and} \quad R^{[k]}(s) \equiv R(s) \cdot R(s-1) \cdots R(s-k+1).$$

Applying the inverse Mellin transforms, we have the approximated differential electron spectrum $\pi_n(\kappa, t)$ as

$$\kappa\pi_n(\kappa, t) = \sum_{k=0}^n {}_nC_k \frac{t^k}{n^k} \frac{1}{2\pi i} \int_{\sigma-i\infty}^{\sigma+i\infty} \left(\frac{\kappa_0}{\kappa}\right)^s R_{1,2}^{[k]}(s) ds,$$

where $R_{1,2}^{[k]}(s)$ denotes the 1,2 element of $R^{[k]}(s)$.

$R^{[k]}(s)$ have poles at $s = -1, 0, k-2$, so we have the differential energy spectrum of electron,

$$\kappa\pi_n(\kappa, t) = \sum_{k=1}^n {}_nC_k \frac{t^k}{n^k} \left\{ \left(\frac{\kappa_0}{\kappa}\right)^{k-2} \rho_{1,2}^{[k]}(k-2) + \rho_{1,2}^{[k]}(0) + \frac{\kappa}{\kappa_0} \rho_{1,2}^{[k]}(-1) \right\},$$

using residues $\rho_{1,2}^{[k]}(s)$ at s .

s	residues $\rho_{1,2}^{[k]}(s)$
-1	$(-1)^{k+1} 2k(k+1)/3$
0	$(-1)^k 2k(k-1)/3$
$k-2$	$(-1)^{k+1} 2k/3$

Exact solutions for the differential spectra and the transition curves

At the limit of $n \rightarrow \infty$, we have the exact solution for the differential electron spectrum $\pi(\kappa, t)$.

The differential spectra and the integral spectra of electron components and photon components for gamma-initiated shower so obtained are

$$\kappa\pi(\kappa, t) = \frac{2}{3} \left(t - \frac{t-2}{\kappa_0/\kappa} \right) te^{-t} + \frac{2}{3} \frac{\kappa t}{\kappa_0} e^{-\kappa_0 t/\kappa},$$

$$\kappa\gamma(\kappa, t) = \kappa\delta(\kappa - \kappa_0)e^{-t} + \frac{t}{3} \left(t - \frac{t-2}{\kappa_0/\kappa} \right) e^{-t} - \frac{2}{3} \frac{\kappa t}{\kappa_0} e^{-\kappa_0 t/\kappa},$$

$$\Pi(\kappa, t) = \frac{2}{3}t \left\{ (2-t)\left(1 - \frac{\kappa}{\kappa_0}\right)e^{-t} + te^{-t} \ln \frac{\kappa_0}{\kappa} + E_2(t) - \frac{\kappa}{\kappa_0} E_2\left(\frac{\kappa_0 t}{\kappa}\right) \right\},$$

$$\Gamma(\kappa, t) = e^{-t} + \frac{t}{3} \left\{ (2-t)\left(1 - \frac{\kappa}{\kappa_0}\right)e^{-t} + te^{-t} \ln \frac{\kappa_0}{\kappa} + 2E_2(t) - \frac{2\kappa}{\kappa_0} E_2\left(\frac{\kappa_0 t}{\kappa}\right) \right\},$$

where $E_2(z)$ denotes the exponential integral function,

$$E_2(z) \equiv \int_1^\infty \frac{e^{-zt}}{t^2} dt.$$

Differential spectra of electrons and photons for cascades in photon gas

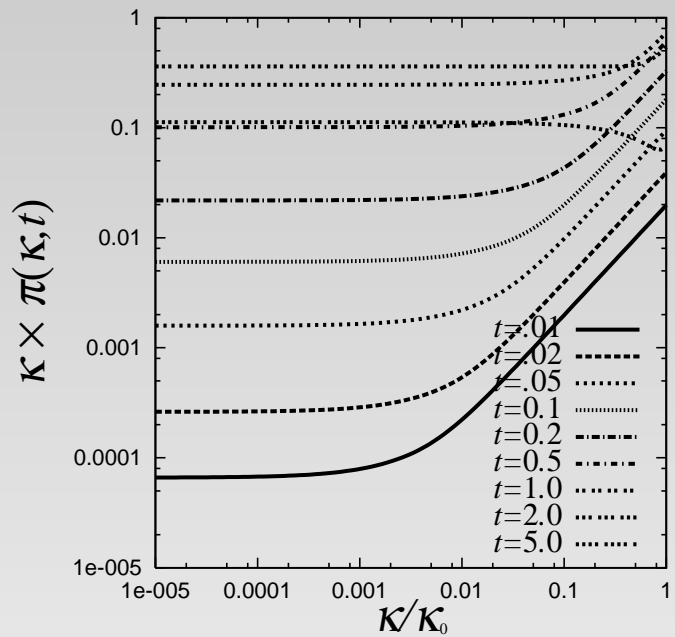


Figure 8: κ -weighted differential energy spectrum of electrons for gamma-initiated showers of energy κ_0 .

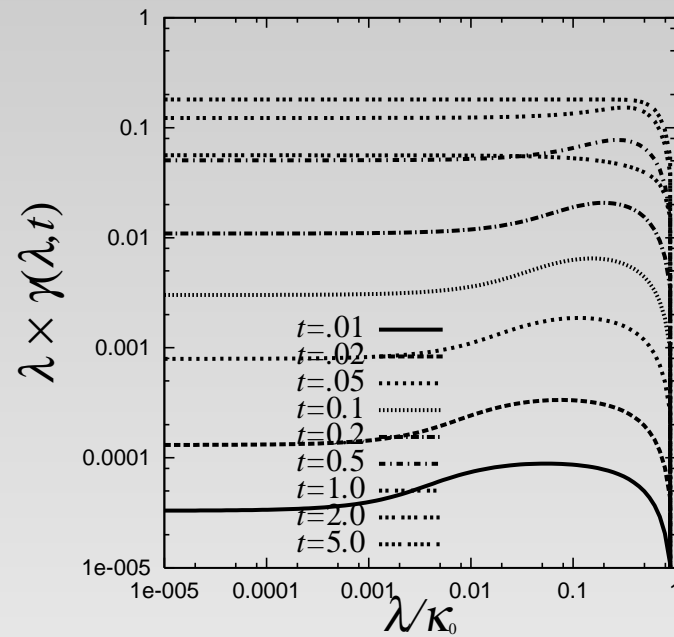


Figure 9: λ -weighted differential energy spectrum of photon for gamma-initiated showers of energy κ_0 .

Transition curves of electrons and photons for cascades in photon gas

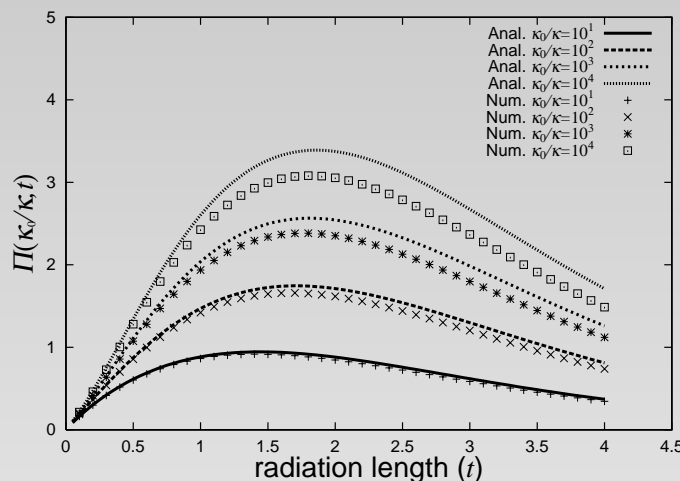


Figure 10: Transition curves of electrons with $\kappa_0/\kappa = 10, 10^2, 10^3, 10^4$ for gamma-initiated showers of energy κ_0 . Analytical results (linrs) are compared with numerical results(dots).

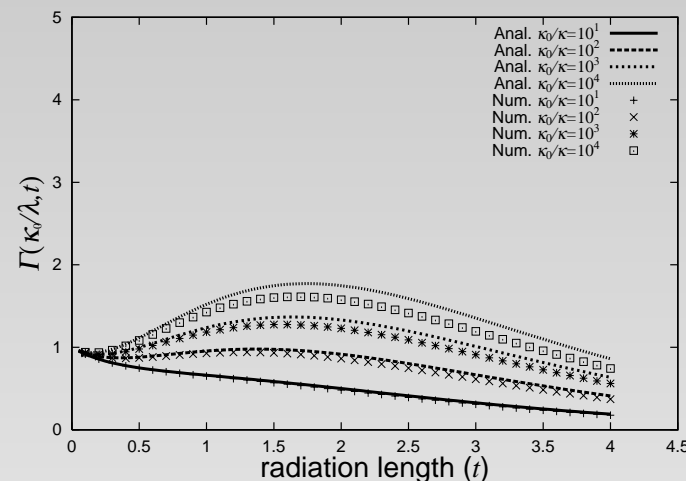


Figure 11: Transition curves of photons with $\kappa_0/\lambda = 10, 10^2, 10^3, 10^4$ for gamma-initiated showers of energy κ_0 . Analytical results (linrs) are compared with numerical results(dots).

Cascades in magnetic field

Akhiezer equation

$$\begin{aligned}\frac{\partial}{\partial t} \pi(E, t) &= -\frac{\pi(E, t)}{(E/W_0)^{1/3}} \int_0^1 \phi(v) dv + \int_E^{W_0} \phi(1 - \frac{E}{E'}) \frac{\pi(E', t)}{(E/W_0)^{1/3}} \frac{dE'}{E'} \\ &\quad + 2 \int_E^{W_0} \psi(\frac{E}{W'}) \frac{\gamma(W', t)}{(W/W_0)^{1/3}} \frac{dW'}{W'}, \\ \frac{\partial}{\partial t} \gamma(W, t) &= \int_W^{W_0} \phi(\frac{W}{E'}) \frac{\pi(E', t)}{(E/W_0)^{1/3}} \frac{dE'}{E'} - \frac{\gamma(W, t)}{(W/W_0)^{1/3}} \int_0^1 \psi(u) du,\end{aligned}$$

We approximate the homogenous functions as

$$\phi(v) = \psi(u) = a.$$

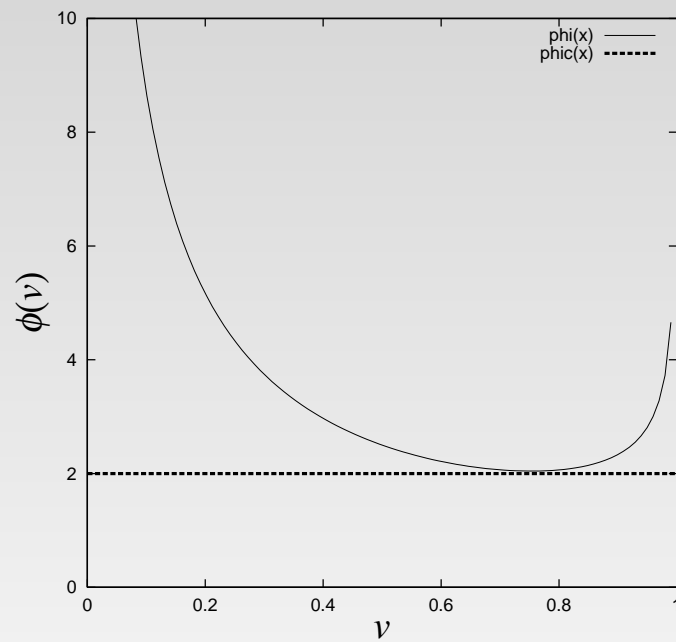


Figure 12: $\phi(v) = 2$.

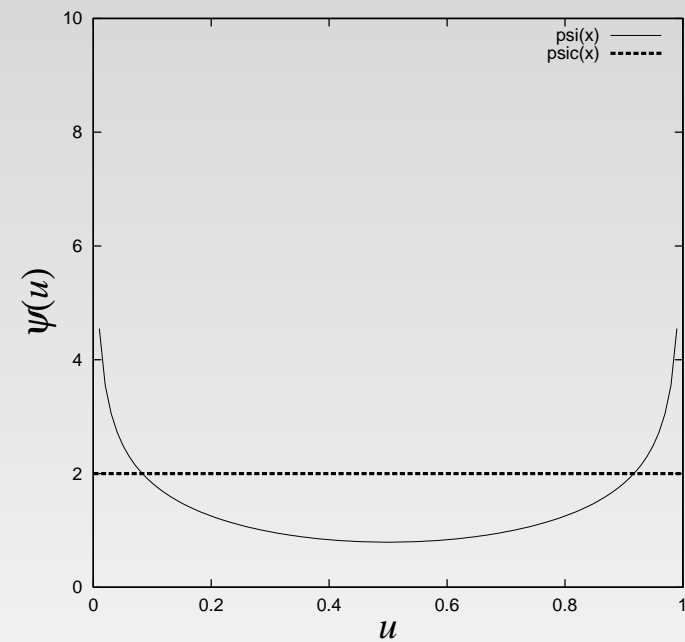


Figure 13: $\psi(u) = 2$.

The differential-difference equations for cascades in the magnetic fields are

$$\frac{\partial}{\partial t} \begin{pmatrix} \mathcal{M}(s, t) \\ \mathcal{N}(s, t) \end{pmatrix} = R(s) \begin{pmatrix} \mathcal{M}(s - 1/3, t) \\ \mathcal{N}(s - 1/3, t) \end{pmatrix}$$

with

$$R(s) \equiv a \begin{pmatrix} -s/(s+1) & 2/(s+1) \\ 1/(s+1) & -1 \end{pmatrix},$$

Then we have the Mellin transform functions,

$$\begin{pmatrix} \mathcal{M}(s, t) \\ \mathcal{N}(s, t) \end{pmatrix} = \sum_{k=0}^{\infty} \frac{t^k}{k!} R^{[k, 1/3]}(s) \begin{pmatrix} \mathcal{M}(s - k/3, 0) \\ \mathcal{N}(s - k/3, 0) \end{pmatrix},$$

where

$$R^{[0, 1/3]}(s) \equiv 1, \quad \text{and} \quad R^{[k, 1/3]}(s) \equiv R(s) \cdot R(s - 1/3) \cdots R(s - [k - 1]/3).$$

Applying the inverse Mellin transforms, we have the differential electron spectrum $\pi(E, t)$ for gamma-initiated shower as

$$E\pi(E, t) = \sum_{k=0}^{\infty} \frac{t^k}{k!} \frac{1}{2\pi i} \int_{\sigma-i\infty}^{\sigma+i\infty} \left(\frac{W_0}{E} \right)^s R_{1,2}^{[k, 1/3]}(s) ds,$$

where $R_{1,2}^{[k, 1/3]}(s)$ denotes the 1,2 element of $R^{[k, 1/3]}(s)$.

residues $\rho_{1,2}^{[k,1/3]}(s)$ in magnetic fields

$R_{1,2}^{[k,1/3]}(s)$ have poles at $s = -1, -2/3, \dots, 2/3$ and
 $s = (k-6)/3, (k-5)/3, (k-4)/3.$

s	residues $\rho_{1,2}^{[k,1/3]}(s)$
-1	$(-1)^{k+1}(2/3)a^k k(k+1)\cdots(k+5)/360$
-2/3	$(-1)^k(2/3)a^k(k-1)k\cdots(k+4)/72$
-1/3	$(-1)^{k+1}(2/3)a^k(k-2)(k-1)\cdots(k+3)/36$
0	$(-1)^k(2/3)a^k(k-3)(k-2)\cdots(k+2)/36$
1/3	$(-1)^{k+1}(2/3)a^k(k-4)(k-3)\cdots(k+1)/72$
2/3	$(-1)^k(2/3)a^k(k-5)(k-4)\cdots k/36$
$(k-6)/3$	$(-1)^{k+1}(2/3)a^k k(k-1)(k-2)/6$
$(k-5)/3$	$(-1)^k(2/3)a^k(k+1)k(k-1)/3$
$(k-4)/3$	$(-1)^{k+1}(2/3)a^k(k+2)(k+1)k/6$

Exact solutions for the differential spectra and the transition curves

The differential spectra and the integral spectra of electron components and photon components for gamma-initiated shower so obtained are

$$\begin{aligned} & E\pi(E, t) \\ = & (2/3)(W_0/E)^{-1}x(720 - 1800x + 1200x^2 - 300x^3 + 30x^4 - x^5)e^{-x}/360 \\ + & (2/3)(W_0/E)^{-2/3}x^2(360 - 480x + 180x^2 - 24x^3 + x^4)e^{-x}/72 \\ + & (2/3)(W_0/E)^{-1/3}x^3(120 - 90x + 18x^2 - x^3)e^{-x}/36 \\ + & (2/3)x^4(30 - 12x + x^2)e^{-x}/36 \\ + & (2/3)(W_0/E)^{1/3}x^5(6 - x)e^{-x}/72 \\ + & (2/3)(W_0/E)^{2/3}x^6e^{-x}/360 \\ + & (2/3)(W_0/E)^{-1}x^3e^{-y}/6 \\ + & (2/3)(W_0/E)^{-1}x^2(3 - y)e^{-y}/3 \\ + & (2/3)(W_0/E)^{-1}x(6 - 6y + y^2)e^{-y}/6, \end{aligned}$$

where we define $x \equiv at$ and $y \equiv at(W_0/E)^{1/3}$.

$$\begin{aligned}
& W\gamma(W, t) \\
= & W\delta(W - W_0)e^{-at} \\
+ & (1/3)(W_0/W)^{-1}x(720 - 1800x + 1200x^2 - 300x^3 + 30x^4 - x^5)e^{-x}/360 \\
+ & (1/3)(W_0/W)^{-2/3}x^2(360 - 480x + 180x^2 - 24x^3 + x^4)e^{-x}/72 \\
+ & (1/3)(W_0/W)^{-1/3}x^3(120 - 90x + 18x^2 - x^3)e^{-x}/36 \\
+ & (1/3)x^4(30 - 12x + x^2)e^{-x}/36 \\
+ & (1/3)(W_0/W)^{1/3}x^5(6 - x)e^{-x}/72 \\
+ & (1/3)(W_0/W)^{2/3}x^6e^{-x}/360 \\
- & (2/3)(W_0/W)^{-1}x^3e^{-y}/6 \\
- & (2/3)(W_0/W)^{-1}x^2(3 - y)e^{-y}/3 \\
- & (2/3)(W_0/W)^{-1}x(6 - 6y + y^2)e^{-y}/6,
\end{aligned}$$

$$\begin{aligned}
& \Pi(E, t) \\
&= (2/3)(1 - E/W_0)x(720 - 1800x + 1200x^2 - 300x^3 + 30x^4 - x^5)e^{-x}/360 \\
&+ \{1 - (E/W_0)^{2/3}\}x^2(360 - 480x + 180x^2 - 24x^3 + x^4)e^{-x}/72 \\
&+ 2\{1 - (E/W_0)^{1/3}\}x^3(120 - 90x + 18x^2 - x^3)e^{-x}/36 \\
&+ (2/3)\ln(W_0/E)x^4(30 - 12x + x^2)e^{-x}/36 \\
&+ 2\{(W_0/E)^{1/3} - 1\}x^5(6 - x)e^{-x}/72 \\
&+ \{(W_0/E)^{2/3} - 1\}x^6e^{-x}/360 \\
&+ x(12 - 12x + 20x^2 + 11x^3 + x^4)e^{-x}/18 \\
&- (E/W_0)x(2 + 2x - 4y + x^2/3 - 2xy + 5y^2 - x^2y/6 + 2xy^2 + x^2y^2/6)e^{-y}/3 \\
&- x^4(30 + 12x + x^2)(E_1(x) - E_1(y))/18,
\end{aligned}$$

$$\begin{aligned}
& \Gamma(W, t) \\
&= e^{-at} \\
&+ (1/3)(1 - W/W_0)x(720 - 1800x + 1200x^2 - 300x^3 + 30x^4 - x^5)e^{-x}/360 \\
&+ (1/2)\{1 - (W/W_0)^{2/3}\}x^2(360 - 480x + 180x^2 - 24x^3 + x^4)e^{-x}/72 \\
&+ \{1 - (W/W_0)^{1/3}\}x^3(120 - 90x + 18x^2 - x^3)e^{-x}/36 \\
&+ (1/3)\ln(W_0/W)x^4(30 - 12x + x^2)e^{-x}/36 \\
&+ \{(W_0/W)^{1/3} - 1\}x^5(6 - x)e^{-x}/72 \\
&+ (1/2)\{(W_0/W)^{2/3} - 1\}x^6e^{-x}/360 \\
&- x(12 - 12x + 20x^2 + 11x^3 + x^4)e^{-x}/18 \\
&+ (W/W_0)x(2 + 2x - 4y + x^2/3 - 2xy + 5y^2 - x^2y/6 + 2xy^2 + x^2y^2/6)e^{-y}/3 \\
&+ x^4(30 + 12x + x^2)(E_1(x) - E_1(y))/18,
\end{aligned}$$

where $E_1(x) \equiv \int_1^\infty t^{-1}e^{-xt}dt$ denotes the exponential integral function.

Differential spectra of electrons and photons for cascades in magnetic field

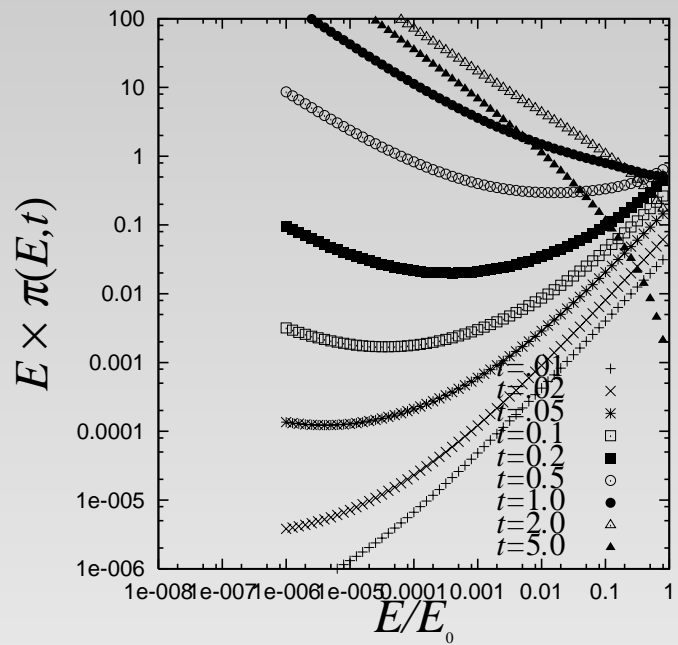


Figure 14: E -weighted differential energy spectrum of electrons for gamma-initiated showers of energy W_0 .

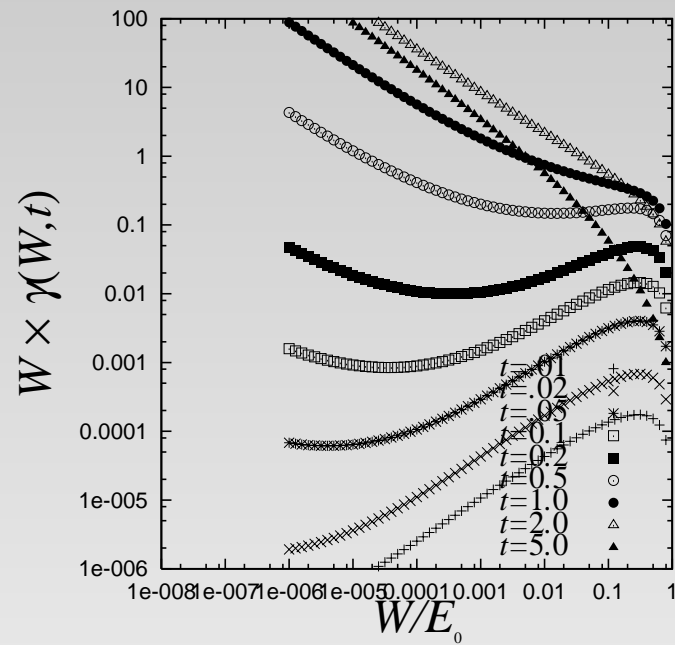


Figure 15: W -weighted differential energy spectrum of photon for gamma-initiated showers of energy W_0 .

Transition curves of electrons and photons for cascades in magnetic field

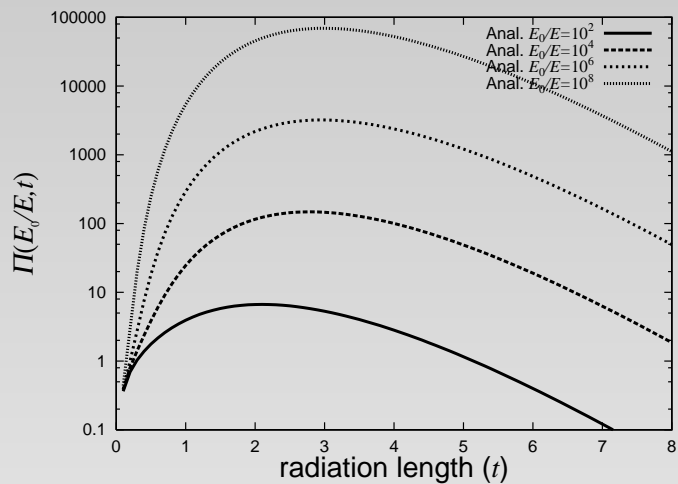


Figure 16: Transition curves of electrons with $W_0/E = 10, 10^2, 10^3, 10^4$ for gamma-initiated showers of energy W_0 .

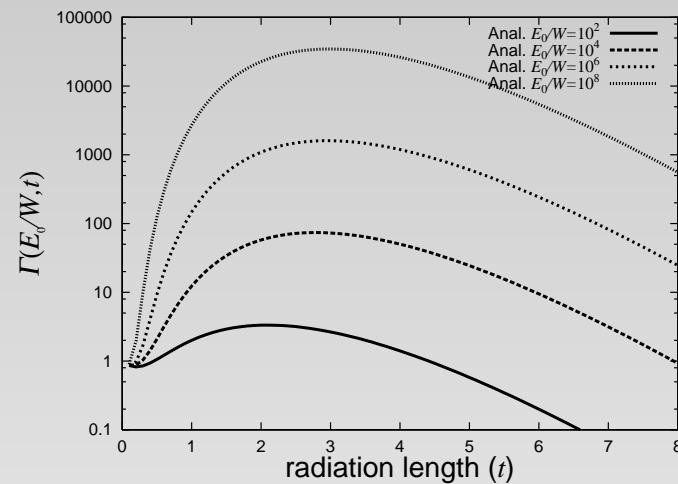


Figure 17: Transition curves of photons with $W_0/W = 10, 10^2, 10^3, 10^4$ for gamma-initiated showers of energy W_0 .

IACTs データに磁場力スケード型スペクトルを探す

- 簡略化断面積で計算した磁場シャワーでは発達の深さによらず、低エネルギーで微分スペクトルが $-5/3$ 乗を示す。
- これは $s = 2/3$ の極の寄与である。
- この様子は詳しい断面積の数値積分解でも変わらない。

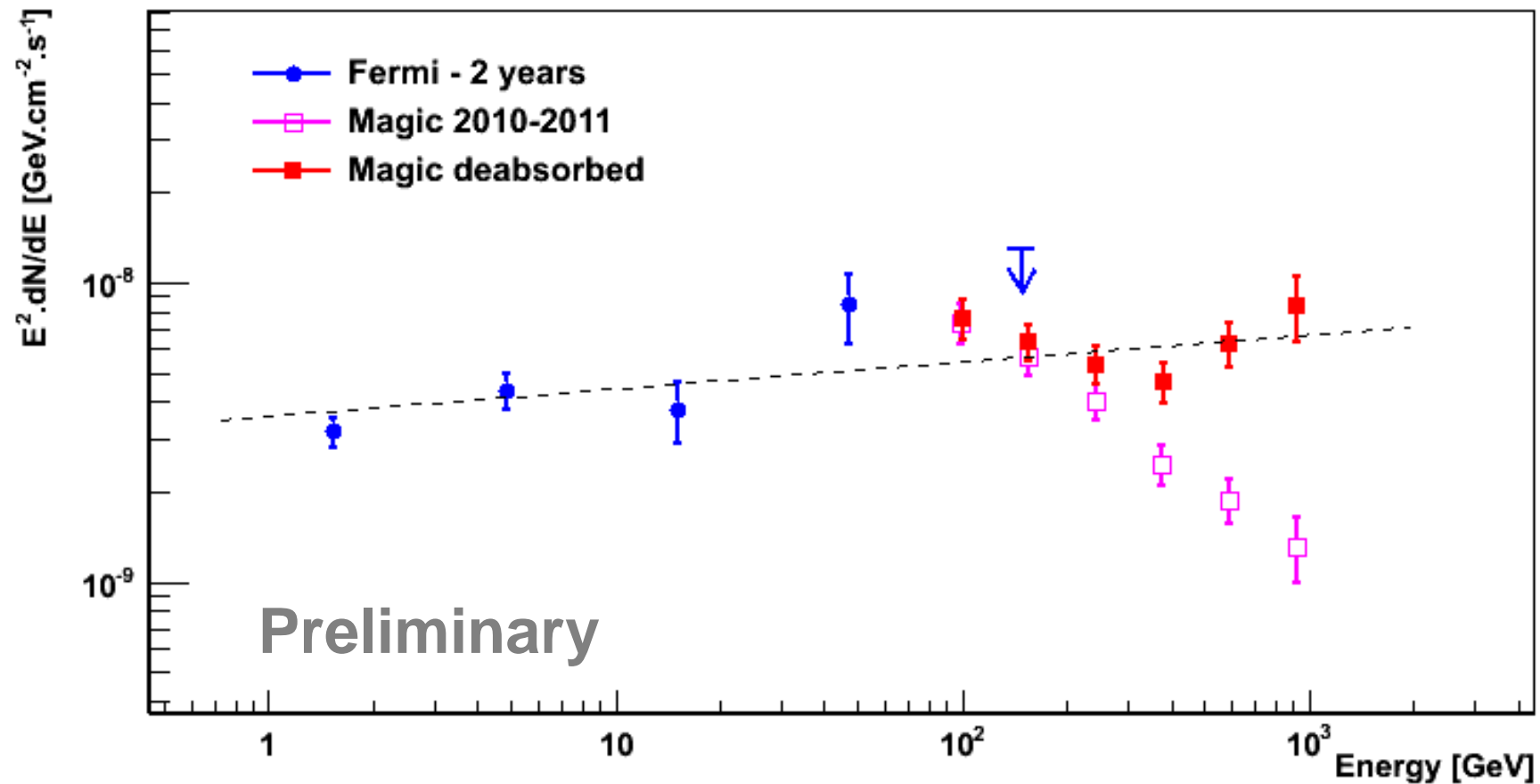
こんなガンマ線天体を探してみる。

ICRC2011 の以下のスライドの中にスペクトルのべきの近いものが見られる、

- P. Colin の Id:1092 のスライド
- F. Aharonian の Invited review talk のスライド

1ES1218+304 SED: 1GeV – 1TeV

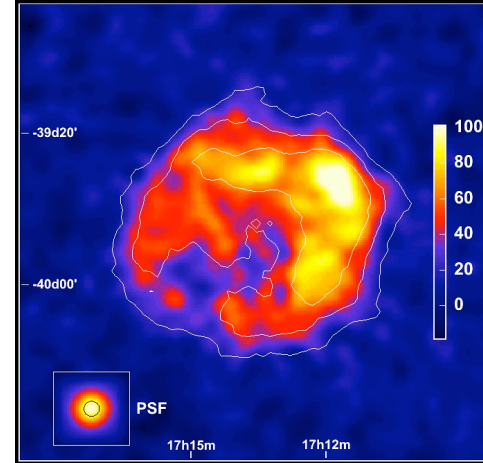
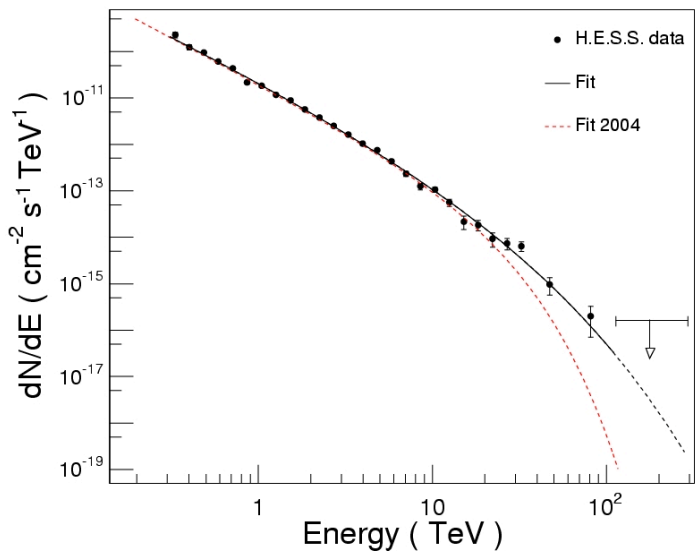
- SED of 1ES1218+304 , 2010-2011 -



The intrinsic spectrum between 1 GeV and 1 TeV
can be well described by a pure power-law (index ~ 1.9)

RXJ1713.7-4639

TeV γ -rays and shell type morphology:
acceleration of p or e in the shell to
energies exceeding 100TeV



can be explained by γ -rays from $pp \rightarrow \pi^0 \rightarrow 2\gamma$

$$\text{HESS: } dN/dE = K E^{-\alpha} \exp[-(E/E_0)^\beta]$$

$$\alpha = 2.0 \quad E_0 = 17.9 \text{ TeV} \quad \beta = 1$$

$$\alpha = 1.79 \quad E_0 = 3.7 \text{ TeV} \quad \beta = 0.5$$

with just "right" energetics:
 $W_p = 10^{50} (n/1\text{cm}^{-3})^{-1} \text{ erg/cm}^3$

(e.g. Berezhko et al, Blasi et al 2007+)

but IC models generally are more preferred... because of TeV-X correlations (?)

IC origin of g-rays cannot indeed be excluded, but this is not a good argument

磁場、光子ガス、物質中のカスケードのスペクトルの比較

磁場のカスケード(詳しい断面積での数値積分解)

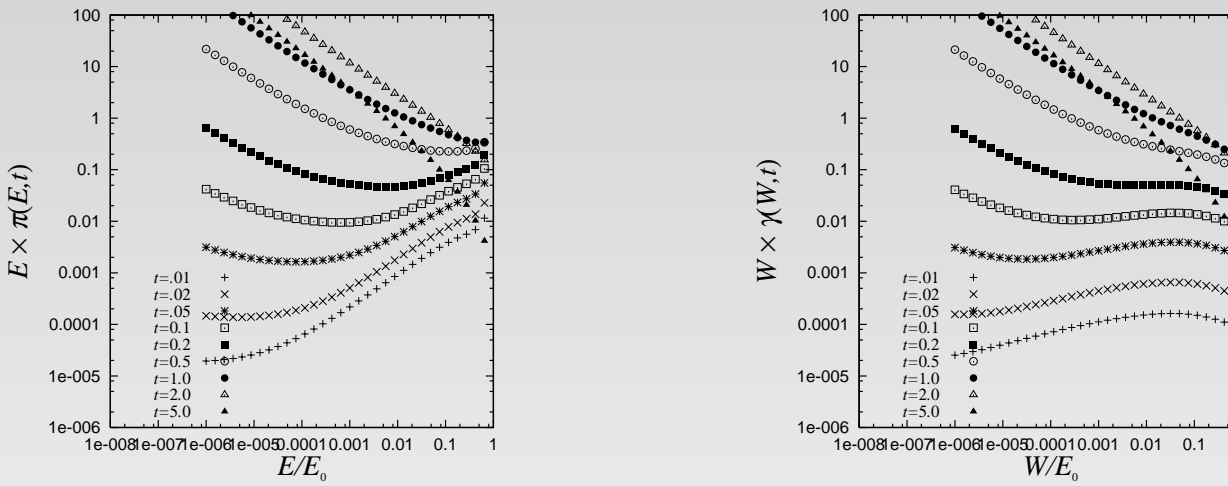


Figure 18: ガンマ入射で磁場の中で発達するカスケードの、電子成分の SED (左) と光子成分の SED(右)。

光子ガス中のカスケード（簡略化断面積での解析解）

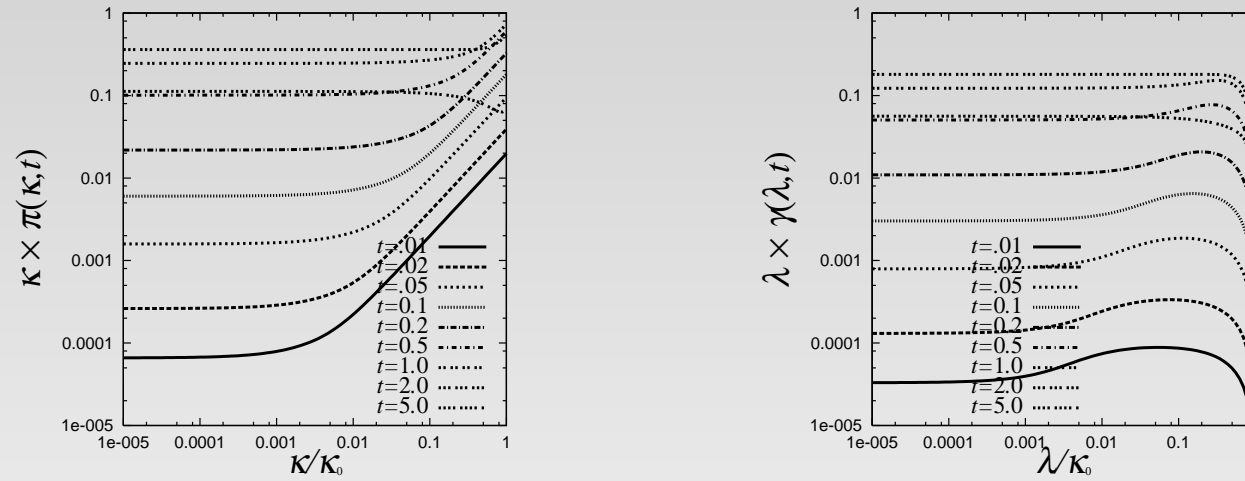


Figure 19: ガンマ入射で光子ガスの中で発達するカスケードの、電子成分の SED (左) と光子成分の SED(右)。

物質中のカスケード(数値積分解)

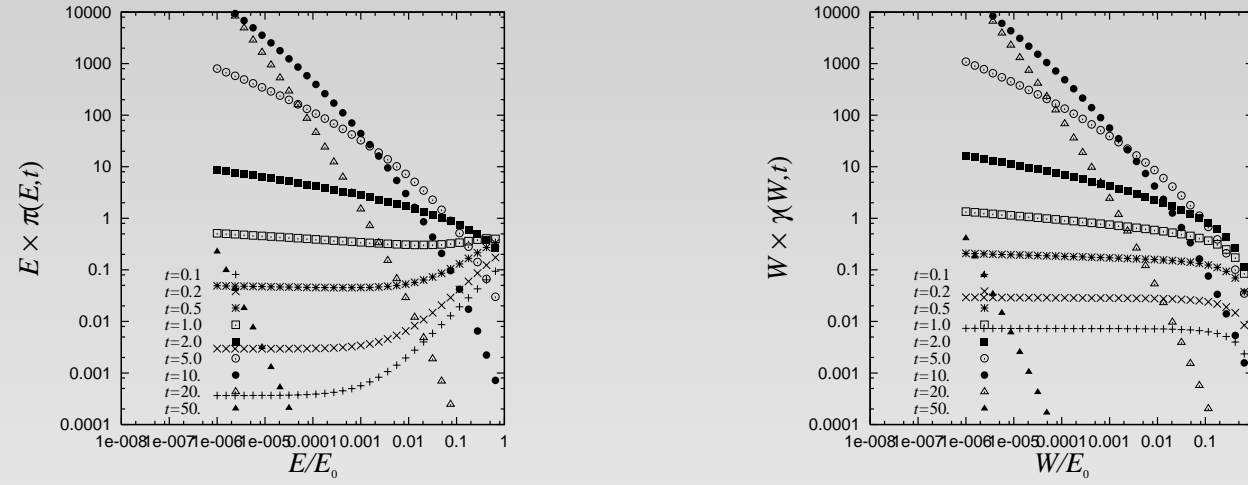


Figure 20: ガンマ入射で物質中で発達するカスケードの、電子成分の SED(左)と光子成分の SED(右)。

簡略化断面積と解析解で開発プログラムを点検

簡略化断面積と解析解の特長

- 厳密解である
- 定性分析が正確で楽
- 極限移行が容易
- 他の開発プログラムの中で断面積を一致させて、正しい結果が出るか確認できる
- 深度刻みやエネルギー刻みなど、シミュレーションパラメタの決定に役立つ

光子ガス、磁場、物質中のカスケードの数値積分解の収束点検

光子ガス中のカスケードの数値積分プログラム

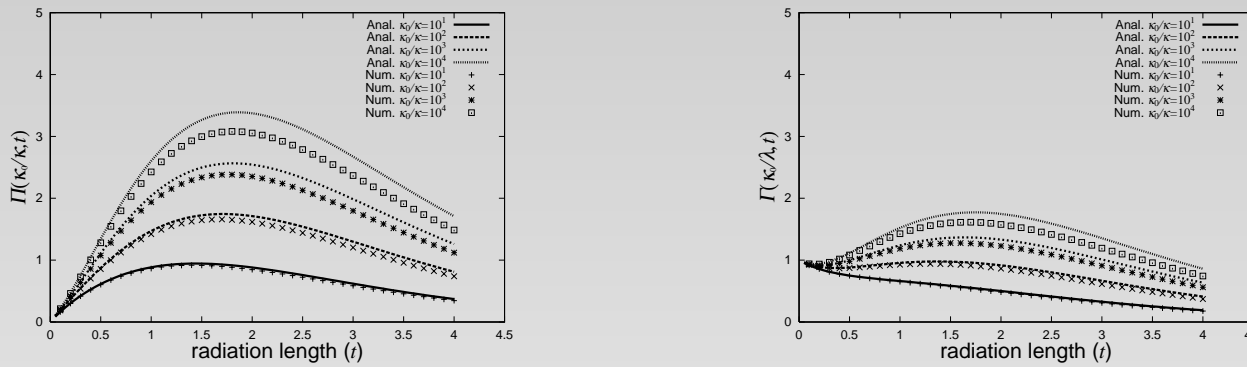


Figure 21: ガンマ入射で光子ガスの中で発達するカスケードの、電子成分の遷移曲線(左)と光子成分の遷移曲線(右)。簡略化断面積での解析解(実線)と数値積分解(点)を比較。。曲線は下から W_0/E または W_0/W で下から $10, 100, 1000, 10000$ 。

磁場のカスケードの数値積分プログラム

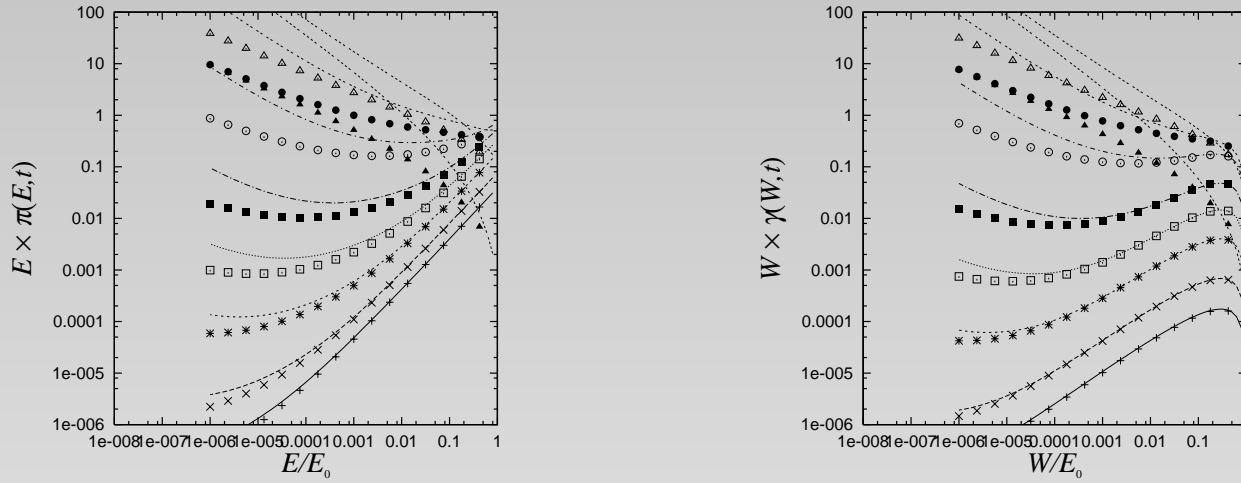


Figure 22: ガンマ入射で磁場の中で発達するカスケードの、電子成分の SED (左) と光子成分の SED(右)。簡略化断面積での解析解 (実線) を同じ断面積での数値積分解 (点) と比較。曲線は下から $t = 0.01, 0.02, 0.05, 0.1, 0.2, 0.5, 1.0, 2.0$ と上昇し、 5.0 では下降している。

物質中のカスケードの数値積分プログラム

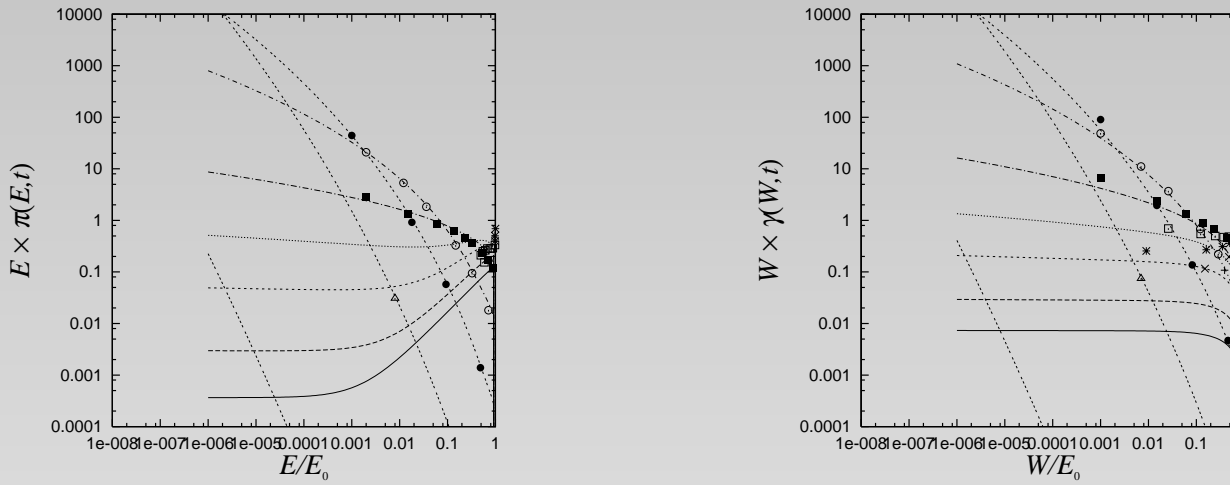


Figure 23: ガンマ入射で物質中で発達するカスケードの、電子成分の SED (左) と光子成分の SED(右)。数値積分解(実線)を Nishimura にある鞍部点法の解をエクセルで簡便計算したもの(点)と比較。曲線は下から $t = 0.1, 0.2, 0.5, 1.0, 2.0, 5.0$ と上昇し、10, 20, 50 では傾きを増加させながら下降している。

結論と議論

- 光子ガスと磁場の中のカスケードについて
 - 詳しい断面積で数値積分法で計算できるようになった。
 - 簡略化断面積で厳密な解析解が得られた。
 - 解析解を得たことで、楽に定性的な分析ができることになった。
- ある種のガンマ線天体について、カスケードの側面から議論できるようになった。
- 簡略化断面積でのシャワーの厳密解は、開発中のプログラムの点検に役立つ。
- 今後簡略化断面積の改良による解析解の質の向上を試みる。